

Multistage Reliability-Based Expansion Planning of AC Distribution Networks Using a Mixed-Integer Linear Programming Model

Alejandra Tabares^a, Gregorio Muñoz-Delgado^b, John F. Franco^c, José M. Arroyo^b, Javier Contreras^b

^a*Department of Electrical Engineering, São Paulo State University, Brazil*

^b*Escuela Técnica Superior de Ingeniería Industrial, Universidad de Castilla-La Mancha, Spain*

^c*School of Energy Engineering, São Paulo State University, Brazil*

Abstract

A new mathematical model for the multistage distribution network expansion planning problem considering reliability is proposed in this paper. Decisions related to substation and branch expansion are driven by the minimization of the total cost, which comprises investment and operating costs including the impact of reliability. The proposed model features two main novelties. First, a set of novel algebraic expressions is devised for a standard reliability index, namely the expected energy not supplied. As a result, the dependence of reliability on network topology is explicitly and effectively cast in the mathematical formulation of the planning problem at hand. In addition, the effect of the network is characterized by a computationally efficient piecewise linear representation of the ac power flow model that takes into account both real and reactive power. The resulting optimization problem is formulated as an instance of mixed-integer linear programming, which provides a suitable framework for the attainment of high-quality solutions with acceptable computational effort using efficient off-the-shelf software with well-known convergence properties. The effectiveness of the proposed planning methodology is empirically demonstrated by providing cheaper expansion plans that enhance system reliability and by achieving better computational results as compared with state-of-the-art models.

Keywords: AC network model, distribution network expansion planning, mixed-integer linear programming, multistage, reliability.

1. Introduction

Due to the capital intensive nature of the transmission and generation systems and the catastrophic social and environmental consequences of their inadequacy, the assessment of reliability has usually focused on such infrastructures. Nonetheless, the analysis of customer interruption occurrences indicates that service unavailability is mostly related to faults at the distribution system level [1, 2]. System-wide reliability can thus be greatly enhanced by adequately planning distribution network investment decisions. To that end, reliability-based distribution planning models should minimize the duration and frequency of customer interruptions through the improvement of standard reliability assessment indices [2–5]. This paper addresses the incorporation of reliability into multistage distribution network expansion planning.

Email addresses: tabares.1989@gmail.com (Alejandra Tabares), Gregorio.Munoz@uclm.es (Gregorio Muñoz-Delgado), jffranco@gmail.com (John F. Franco), JoseManuel.Arroyo@uclm.es (José M. Arroyo), Javier.Contreras@uclm.es (Javier Contreras)

Existing techniques for reliability assessment can be categorized in two groups, namely simulation-based methods and non-simulation-based approaches. In the former, reliability indices are obtained via examining network operation for every component outage, Monte Carlo simulation being typically adopted [6]. To that end, a power flow is run to determine the impact of every interruption, which is computationally demanding. Moreover, simulation-based methods cannot be directly integrated into the optimization models used for distribution operation and planning, thereby requiring the application of inexact solution techniques wherein reliability assessment is decoupled from the optimization process. Relevant examples are [7–11].

Non-simulation-based methods usually derive the impact range of interruptions through topological analysis [4], or by formulating an interruption incidence matrix based on topological information from distribution networks [12]. Both approaches involve the characterization of the network topology, which, within the context of the optimization problems related to operation and planning, is *a priori* unknown, hence being represented by decision variables. As a result of this topological dependence, the use of non-simulation-based methods for the evaluation of reliability indices within such optimization problems drastically increases their mathematical complexity.

The first non-simulation-based formulation explicitly incorporating reliability assessment into an optimization problem related to distribution networks is presented in [13], which addresses the network reconfiguration problem. Using a fictitious power flow to describe the load nodal affiliation, the effects of failures occurring in the shortest upstream path between each load node and the corresponding substation are quantified, but the effects of fault isolation are disregarded. Hence, following the terminology coined in [14], the non-simulation-based formulation in [13] solely considers repair-and-switching interruptions in the reliability assessment, i.e., switching-only interruptions are neglected. This practical issue is addressed in the linear-programming-based formulation proposed in [14], which, similarly to [13], relies on fictitious power flows. Although this formulation can calculate all load-node and system-level reliability indices, its reliance on the enumeration of all possible component outages can considerably increase the number of decision variables and constraints of the resulting optimization model, which may lead to prohibitive computational effort. In an attempt to reduce the dimension of the formulation presented in [14], an alternative albeit equivalent approach is proposed in [15], whereby reliability indices are represented by a set of recursive algebraic expressions. The previous works [14, 15] calculate the standard system-level reliability indices by modeling the impact of every interruption on load nodes. In [16], a linear-programming-based approach is proposed to obtain such system reliability indices without explicitly formulating the impact of each interruption on node-level reliability indices. The reliability assessment approaches in [14–16] disregard post-fault reconfiguration mechanisms based on the operation of tie switches. This gap is addressed in [17, 18] by the consideration of fault scenarios, thereby requiring the explicit and, hence, computationally expensive characterization of system operation under every component outage, similar to the enumeration-based approach relying on fictitious flows used in [13, 14]. In [17], the reliability assessment is performed taking into account the actions of circuit breakers and switches through a set of linear constraints that determine the post-fault reconfiguration strategies and lead to a reduction in the impact and duration of interruptions. Furthermore, in [18], the model described in [17] is integrated in the circuit breaker and switch allocation problem to account for reliability.

The above findings on non-simulation-based reliability assessment have triggered the development of new approaches for reliability-constrained distribution network expansion planning. The first use of a non-simulation-based approach for the incorporation of reliability into the multistage distribution network expansion planning problem is reported in [19]. In that work, the topology-dependent linear programming formulation for reliability assessment described in [14] is explicitly accommodated in terms of the decision variables of the optimization problem. This approach features

59 a major shortcoming, namely replacing the conventional use of simulation with the enumeration-
60 based expressions of [19] may lead to intractability due to the large dimension of the resulting
61 planning problem. Attempts to reduce the increase in the size of the planning problem while con-
62 sidering non-simulation-based reliability assessment are presented in [20] and its extended version
63 [21], which also accounts for reliability incentive schemes and distributed generation. However, the
64 problem size reduction is gained at the expense of disregarding switching-only interruptions, thereby
65 potentially leading to an imprecise reliability assessment [16] that may hinder the compliance with
66 standards and regulations. Moreover, previous works [19–21] rely on an approximate network model
67 based on a constant power factor across the system, which can give rise to optimistic planning so-
68 lutions or even impractical investment decisions eventually requiring load shedding. Both modeling
69 simplifications are recently addressed in [22, 23] by adopting the enumerative scenario-based rela-
70 bility assessment formulation of [17] and an approximate ac network model. Unfortunately, in [22],
71 a static approach is adopted, which may lead to oversized expansion plans, as shown in [24], whereas
72 practical network-related aspects such as losses and current limits are neglected. The enumeration-
73 based model presented in [22] is extended to a multistage setting in [23]. However, such an extended
74 modeling capability yields prohibitively large optimization problems, thereby requiring the adoption
75 of practical simplifications related to network topology, transfer nodes, and demand.

76 Motivated by the issues of existing works, this paper presents a new non-simulation-based ap-
77 proach for the precise incorporation of reliability into multistage distribution network expansion
78 planning. Within the context of reliability-constrained distribution network expansion planning
79 [7–11, 19–23], the proposed approach features two main novelties:

- 80 1. The modeling of reliability using both a set of algebraic expressions built on the formulation
81 described in [15] and a set of radiality constraints, which have been adapted from [25] for the
82 planning problem at hand.
- 83 2. The characterization of the effect of the distribution network using the accurate linearized ac
84 load flow presented in [24].

85 Compared with existing works on non-simulation-based reliability assessment [13–18], the nov-
86 elty of the proposed approach lies not only in the incorporation of investment decisions and system
87 operation, which are disregarded therein, but also in the reliability model itself. Major distinctive
88 aspects include 1) the consideration of switching-only interruptions, which are neglected in [13],
89 2) the characterization of the dependence of reliability on the *a priori* unknown network topol-
90 ogy, which is not featured in [13–15], 3) the reliance on simple recursive algebraic nodal expressions,
91 unlike [13, 14, 16–18], and 4) in contrast to [13, 14, 17, 18], the use of a non-enumerative formulation.

92 It should be noted that the explicit representation of reliability as part of the problem formu-
93 lation renders the proposed model suitable for non-heuristic techniques, which is a relevant salient
94 feature over previous approximate approaches for distribution network expansion planning relying
95 on simulation-based reliability assessment [7–11]. In comparison with recent non-simulation-based
96 reliability-constrained planning formulations [19–23], the benefits associated with the novelties of
97 the proposed approach are related to 1) the modeling of reliability, 2) the characterization of the
98 distribution network, and 3) the decision-making framework.

99 Regarding reliability, unlike [20, 21], switching-only interruptions are precisely considered while
100 1) overcoming the potential intractability of [19, 22, 23] stemming from the explicit representation of
101 system operation for all possible faults at every stage, and 2) accounting for the practical features
102 neglected in [22, 23], namely radial operation under the normal state, transfer nodes, and the
103 chronological aspect of demand for network operation.

104 As for the effect of the distribution network, the proposed approach significantly differs from
105 [8, 11, 19–23] as reactive power is explicitly modeled while considering network losses and current

Table 1: Proposed Approach versus the Related Literature

Feature	[7]	[8]	[9]	[10]	[11]	[19]	[20]	[21]	[22]	[23]	Proposed approach
Mathematical-programming-based	×	×	×	×	×	✓	✓	✓	✓	✓	✓
AC power flow	✓	×	✓	✓	×	×	×	×	✓	✓	✓
Non-enumerative reliability assessment	×	×	×	×	×	×	✓	✓	×	×	✓
Switching-only interruptions	×	✓	✓	✓	✓	✓	×	×	✓	✓	✓
Multistage	✓	✓	✓	✓	✓	✓	✓	✓	×	✓	✓
Radiality	✓	✓	×	✓	✓	✓	✓	✓	×	×	✓
Load levels	✓	✓	×	✓	✓	✓	✓	✓	×	×	✓
Active power losses	✓	✓	×	✓	✓	✓	×	×	×	×	✓
Current limits	✓	✓	×	✓	✓	✓	×	✓	×	×	✓
Transfer nodes	×	×	×	×	✓	✓	✓	✓	×	×	✓

106 limits, thereby providing a more accurate and practical characterization. Moreover, in contrast to
 107 the static planning framework adopted in [22], the timing of investment decisions is an outcome of
 108 the optimization process.

109 Table 1 summarizes the main differences between this work and the state of the art of reliability-
 110 constrained distribution network expansion planning [7–11, 19–23]. In this table, symbols “✓” and
 111 “×” respectively indicate whether a particular aspect is considered or not. As can be observed, the
 112 proposed approach substantially departs from the relevant body of literature [7–11, 19–23] in both
 113 modeling and methodological features.

114 The main contributions of this work are twofold:

- 115 1. From a modeling perspective, an explicit non-enumeration-based formulation is presented,
 116 for the first time in the literature, for multistage reliability-constrained distribution network
 117 expansion planning with an ac power flow model and radiality constraints. Unlike previ-
 118 ously reported works, the novel ac-based planning model benefits from the availability of
 119 effective mathematical programming techniques and the more precise representation of dis-
 120 tribution network operation including radiality, losses, current limits, and different loading
 121 conditions. Moreover, the proposed planning model features a novel mathematical charac-
 122 terization of reliability assessment that overcomes the potential intractability of the state-of-
 123 the-art enumeration-based formulations while accounting for the effect of transfer nodes and
 124 switching-only interruptions.
- 125 2. From a methodological point of view, the multistage distribution network expansion planning
 126 problem is addressed by an accurate approach based on mixed-integer linear programming con-
 127 sidering technical, economic, and reliability aspects. The superiority of the proposed method
 128 is backed by its computationally effective ability to optimally solve cases for which the state-
 129 of-the-art formulations require substantially longer computing times to identify lower-quality
 130 and even infeasible solutions.

131 To the best of our knowledge, there is no current literature contribution on multistage reliability-
 132 constrained distribution network expansion planning using a mixed-integer linear programming
 133 framework to jointly and effectively consider 1) a precise power flow model including reactive power,
 134 losses, and current limits, 2) radial operation under the normal state, 3) the impact of transfer nodes
 135 and switching-only interruptions on reliability, and 4) the chronological characterization of demand
 136 for network operation. Thus, both contributions constitute an original and effective solution to the
 137 major issues of the state of the art [7–11, 19–23], which may lead to intractability, suboptimality,
 138 and even impractical solutions.

139 The remainder of this paper is organized as follows. Section 2 is devoted to distribution network
140 reliability assessment. Section 3 presents the problem formulation. In Section 4, numerical results
141 are reported and analyzed. Relevant conclusions are drawn in Section 5. Finally, the nomenclature
142 and the linearization schemes used in Section 3 are described in Appendices A and B, respectively.

143 2. Distribution Network Reliability Assessment

144 The proposed approach relies on the analytical predictive reliability assessment described in
145 [1, 4, 5] for standard reliability metrics such as expected energy not supplied (EENS), system aver-
146 age interruption frequency index (SAIFI), and system average interruption duration index (SAIDI),
147 among others [3]. Thus, the effect of component outages is characterized using two pieces of infor-
148 mation, namely failure rates and interruption durations.

149 As is done in [14, 15], it is considered that 1) the resulting meshed network operates radially,
150 2) every branch has a switch, 3) at the output of each substation, the feeder is equipped with a
151 circuit breaker without a recloser, 4) interruptions are caused by the sustained outage of individual
152 branches, and 5) the healthy part of the system can be re-energized after fault isolation.

153 In the occurrence of a fault, the circuit breaker in the feeder of the branch involved is opened,
154 affecting all the nodes belonging to the feeder. Then, the system is reconfigured in order to minimize
155 the energy not supplied. More specifically, the loads located upstream of the fault are re-energized
156 by opening the first switch upstream of the fault followed by the closing of the feeder circuit breaker.
157 After the cause of the fault is eliminated, the corresponding switch is closed and service is fully
158 restored.

159 As a consequence, load nodes are affected by switching-only interruptions and repair-and-
160 switching interruptions [14, 15]. Switching-only interruptions are associated with reconfiguring
161 the network to isolate a damaged component. Repair-and-switching interruptions correspond to
162 those for which the supply is not restored until the damage is repaired.

163 Both types of nodal interruptions are characterized by the corresponding expected rates and du-
164 rations. Such magnitudes depend solely on the information related to branches, i.e., lengths, failure
165 rates, and durations of repair-and-switching and switching-only interruptions [14, 15]. Therefore,
166 using the expected nodal interruption rates and durations, the standard reliability metrics can be
167 calculated as described in [14, 15].

168 It is worth mentioning that the above reliability-related modeling aspects have been commonly
169 considered in distribution system operation and planning [26]. Within such a context and according
170 to industry practice [27], the reliability worth is estimated based on the costs associated with
171 standard reliability metrics. Here, a widely used reliability index, namely EENS, is adopted to
172 quantify reliability and, hence, investment decisions are driven by the costs due to the unserved
173 energy during contingencies, i.e., the costs of EENS. Note, however, that other practical reliability
174 metrics can be considered.

175 3. Problem Formulation

176 Using the notation described in Appendix A, this section presents the mathematical model
177 proposed for multistage reliability-constrained distribution network expansion planning, which is a
178 challenging instance of mixed-integer nonlinear programming [28]. The application of the lineariza-
179 tion schemes provided in Appendix B eventually yields a mixed-integer linear programming model.
180 As a result, finite convergence to the global optimum is guaranteed, while a measure of the distance
181 to optimality is readily available [29].

182 As done in the closely related literature [7–11, 19–23], the model assumes that future nodal peak
183 demands are obtained from appropriate forecasting procedures that are beyond the scope of this
184 paper. For further details, the interested reader is referred to the recent survey provided in [30].

185 *3.1. Objective Function*

186 As is customary in industry practice [27] and the relevant literature on multistage distribution
 187 network expansion planning [7–9, 11, 19–21, 23], the objective of the proposed model is to minimize
 188 the present value of the total cost, which comprises investment and operating costs. The operating
 189 cost includes maintenance, energy production, load shedding, and reliability costs, the latter being
 190 modeled here by the costs of EENS, as explained in Section 2. Mathematically, the economic goal
 191 of the proposed optimization is formulated as:

$$\begin{aligned} \text{Minimize } c^{PV} &= \sum_{y \in \mathcal{Y}} \frac{(1 + I_r)^{-y}}{I_r} c_y^I + \sum_{y \in \mathcal{Y}} \left[(1 + I_r)^{-y} \left(c_y^M + c_y^E + c_y^{Sh} + c_y^{EENS} \right) \right] + \\ &\frac{(1 + I_r)^{-|\mathcal{Y}|}}{I_r} \left(c_{|\mathcal{Y}|}^M + c_{|\mathcal{Y}|}^E + c_{|\mathcal{Y}|}^{Sh} + c_{|\mathcal{Y}|}^{EENS} \right). \end{aligned} \quad (1)$$

192 As done in [8, 11, 19], the present value of the total cost c^{PV} is modeled in (1) under the
 193 hypothesis of a perpetual or infinite planning horizon [31], i.e., the investment is amortized an-
 194 nually throughout the lifetime of the installed equipment and after its lifetime expiration there is
 195 a reinvestment in the same type of equipment. Thus, according to [31], the present value of the
 196 total cost minimized in (1) is equal to the sum of the present value of the total investment cost,
 197 represented by the first summation term in (1), and the present value of the total operating cost,
 198 which is characterized by the remaining terms in (1). Note that the last term in (1) solely involving
 199 operating costs at the last planning stage represents the perpetual portion of such costs. Individual
 200 cost terms in (1) are cast as follows:

$$\begin{aligned} c_y^I &= RR^S \sum_{i \in SN} \left(C_i^{I,S} x_{i,y}^S + \sum_{t \in \mathcal{T}} C_t^{I,T} x_{i,t,y}^T \right) + \\ &RR^B \left(\sum_{ij \in AB} \sum_{c \in \mathcal{C}} C_{ij,c}^{I,AB} x_{ij,c,y}^{AB} + \sum_{ij \in RB} \sum_{\substack{c \in \mathcal{C} \\ c \neq \beta^{RB}}} C_{ij,c}^{I,RB} x_{ij,c,y}^{RB} \right); \forall y \in \mathcal{Y} \end{aligned} \quad (2)$$

$$c_y^M = \sum_{i \in SN} C_i^{M,S} w_{i,y}^{S,ex} + \sum_{i \in SN} \sum_{t \in \mathcal{T}} C_t^{M,T} w_{i,t,y}^T + \sum_{ij \in B} \sum_{c \in \mathcal{C}} C_{ij,c}^{M,B} w_{ij,c,y}^B; \forall y \in \mathcal{Y} \quad (3)$$

$$c_y^E = \sum_{l \in \mathcal{L}} \Delta_l \left(\sum_{i \in SN} C_{i,l}^E P_{i,l,y}^S \right); \forall y \in \mathcal{Y} \quad (4)$$

$$c_y^{Sh} = \sum_{l \in \mathcal{L}} \Delta_l \left(\sum_{i \in SN} C_{i,l}^{Sh} P_{i,l,y}^{Sh} \right); \forall y \in \mathcal{Y} \quad (5)$$

$$c_y^{EENS} = C^{EENS} EENS_y; \forall y \in \mathcal{Y}. \quad (6)$$

202 In (2), the amortized cost of the investment at each stage is formulated as the sum of the
 203 costs associated with the reinforcement and construction of substations, and the replacement and
 204 addition of branches. The capital recovery rates for substations and circuits are computed as
 205 $RR^S = \frac{I_r(1+I_r)^{\eta^S}}{(1+I_r)^{\eta^S}-1}$ and $RR^B = \frac{I_r(1+I_r)^{\eta^B}}{(1+I_r)^{\eta^B}-1}$, respectively. Expressions (3) model the maintenance
 206 costs of existing substations, newly added transformers, and branches at each stage. The cost of
 207 energy production at each stage is modeled in (4). Using a sufficiently large penalty cost coefficient,
 208 C^{Sh} , load shedding costs are formulated in (5). Finally, reliability costs, i.e., the costs of expected

209 energy not supplied along the planning horizon, are cast in (6). Based on [7, 9, 11, 19, 20, 23],
 210 for each stage y , the reliability cost is equal to the cost coefficient for EENS, C^{EENS} , times the
 211 expected energy not supplied at that stage, $EENS_y$. According to [1], the calculation of EENS
 212 involves products of two terms, namely 1) the expected duration of the interruptions experienced by
 213 load nodes, and 2) the corresponding average load curtailment. As described in Section 2, branch
 214 outages give rise to the curtailment of nodal demands with two different durations depending on
 215 whether switching or repair-and-switching actions are implemented. Thus, the levels of expected
 216 energy not supplied along the planning horizon are formulated as follows [14–19, 23]:

$$EENS_y = \sum_{i \in \mathcal{N}} (\Gamma_{i,y}^{RS} + \Gamma_{i,y}^{SO}) \sum_{l \in \mathcal{L}} \frac{\Delta_l F_l^D P_{i,y}^D}{8760}; \forall y \in \mathcal{Y} \quad (7)$$

217 where the term within parentheses represents expected nodal interruption durations whereas the
 218 other term is related to nodal load curtailment. Note that the effect of branch outages on both
 219 interruption durations is precisely formulated in Section 3.6. As for load curtailment, the seasonal or
 220 chronological aspect of demand is modeled by the discretization of the annual system load-duration
 221 curve into a set of blocks each characterized by its load level and duration. Furthermore, for the
 222 sake of simplicity, such a system-wide demand characterization is applied on a nodal basis.

223 3.2. Investment and Operational Constraints

Based on [8, 11, 19, 32], investment and operational variables are constrained by (8)–(30):

$$\sum_{y \in \mathcal{Y}} \sum_{c \in \mathcal{C}} x_{ij,c,y}^{AB} \leq 1; \forall ij \in \mathcal{AB} \quad (8)$$

$$\sum_{y \in \mathcal{Y}} \sum_{c \in \mathcal{C} | c \neq \beta^{RB}} x_{ij,c,y}^{RB} \leq 1; \forall ij \in \mathcal{RB} \quad (9)$$

$$w_{ij,c,y}^B \leq 1; \forall ij \in \mathcal{FB} | \varphi_{ij} = 1, \forall c \in \mathcal{C}, \forall y \in \mathcal{Y} \quad (10)$$

$$w_{ij,c,y}^B \leq \sum_{p=1}^y x_{ij,c,p}^{RB}; \forall ij \in \mathcal{RB} | \varphi_{ij} = 1, \forall c \in \mathcal{C} | c \neq \beta^{RB}, \forall y \in \mathcal{Y} \quad (11)$$

$$w_{ij,c,y}^B \leq 1 - \sum_{p=1}^y \sum_{e \in \mathcal{C} | e \neq \beta^{RB}} x_{ij,e,p}^{RB}; \forall ij \in \mathcal{RB} | \varphi_{ij} = 1, \forall c \in \mathcal{C} | c = \beta^{RB}, \forall y \in \mathcal{Y} \quad (12)$$

$$w_{ij,c,y}^B \leq \sum_{p=1}^y x_{ij,c,p}^{AB}; \forall ij \in \mathcal{AB} | \varphi_{ij} = 1, \forall c \in \mathcal{C}, \forall y \in \mathcal{Y} \quad (13)$$

$$w_{ij,c,y}^B = 1; \forall ij \in \mathcal{FB} | \varphi_{ij} = 0, \forall c \in \mathcal{C}, \forall y \in \mathcal{Y} \quad (14)$$

$$w_{ij,c,y}^B = \sum_{p=1}^y x_{ij,c,p}^{RB}; \forall ij \in \mathcal{RB} | \varphi_{ij} = 0, \forall c \in \mathcal{C} | c \neq \beta^{RB}, \forall y \in \mathcal{Y} \quad (15)$$

$$w_{ij,c,y}^B = 1 - \sum_{p=1}^y \sum_{e \in \mathcal{C} | e \neq \beta^{RB}} x_{ij,e,p}^{RB}; \forall ij \in \mathcal{RB} | \varphi_{ij} = 0, \forall c \in \mathcal{C} | c = \beta^{RB}, \forall y \in \mathcal{Y} \quad (16)$$

$$w_{ij,c,y}^B = \sum_{p=1}^y x_{ij,c,p}^{AB}; \forall ij \in \mathcal{AB} | \varphi_{ij} = 0, \forall c \in \mathcal{C}, \forall y \in \mathcal{Y} \quad (17)$$

$$w_{ij,y}^{B+} + w_{ij,y}^{B-} = \sum_{c \in \mathcal{C}} w_{ij,c,y}^B; \forall ij \in \mathcal{B}, \forall y \in \mathcal{Y} \quad (18)$$

$$w_{ij,c,y}^B = 0; \forall ij \in \mathcal{FB}, \forall c \in \mathcal{C} | c \neq \beta^{FB}, \forall y \in \mathcal{Y} \quad (19)$$

$$\sum_{y \in \mathcal{Y}} x_{i,y}^S \leq 1; \forall i \in \mathcal{SN} \quad (20)$$

$$\sum_{y \in \mathcal{Y}} \sum_{t \in \mathcal{T}} x_{i,t,y}^T \leq 1; \forall i \in \mathcal{SN} \quad (21)$$

$$x_{i,t,y}^T \leq \sum_{p=1}^y x_{i,p}^S; \forall i \in \mathcal{SN}, \forall t \in \mathcal{T}, \forall y \in \mathcal{Y} \quad (22)$$

$$w_{i,t,y}^T \leq \sum_{p=1}^y x_{i,t,p}^T; \forall i \in \mathcal{SN}, \forall t \in \mathcal{T}, \forall y \in \mathcal{Y} \quad (23)$$

$$\sum_{t \in \mathcal{T}} w_{i,t,y}^T \leq 1; \forall i \in \mathcal{SN}, \forall y \in \mathcal{Y} \quad (24)$$

$$x_{i,y}^S, w_{i,y}^{S,ex} \in \{0, 1\}; \forall i \in \mathcal{SN}, \forall y \in \mathcal{Y} \quad (25)$$

$$x_{i,t,y}^T, w_{i,t,y}^T \in \{0, 1\}; \forall i \in \mathcal{SN}, \forall t \in \mathcal{T}, \forall y \in \mathcal{Y} \quad (26)$$

$$x_{ij,c,y}^{RB} \in \{0, 1\}; \forall ij \in \mathcal{RB}, \forall c \in \mathcal{C}, \forall y \in \mathcal{Y} \quad (27)$$

$$x_{ij,c,y}^{AB} \in \{0, 1\}; \forall ij \in \mathcal{AB}, \forall c \in \mathcal{C}, \forall y \in \mathcal{Y} \quad (28)$$

$$w_{ij,c,y}^B \in \{0, 1\}; \forall ij \in \mathcal{B}, \forall c \in \mathcal{C}, \forall y \in \mathcal{Y} \quad (29)$$

$$w_{ij,y}^{B-}, w_{ij,y}^{B+} \in \{0, 1\}; \forall ij \in \mathcal{B}, \forall y \in \mathcal{Y}. \quad (30)$$

224 Expressions (8) and (9) ensure that a maximum of one installation or reinforcement is performed
 225 for each branch throughout the planning horizon. In (10)–(19), branch operation is modeled by
 226 binary variables different from those used to represent investment decisions, which allows handling
 227 radially operated meshed distribution networks. Expressions (10)–(17) guarantee that a branch
 228 with a specific conductor type can be used once its corresponding investment has already been
 229 made. Expressions (10)–(13) are associated with the set of branches that can be switched under
 230 normal operation, for which the corresponding binary parameters φ_{ij} are equal to 1. Analogously,
 231 expressions (14)–(17) are related to non-switchable branches under normal operation, which are
 232 characterized by φ_{ij} equal to 0.

233 The operating state of a given branch ij is represented by two binary variables in (18), as
 234 proposed in [33]. If $w_{ij,y}^{B+}$ or $w_{ij,y}^{B-}$ is equal to 1, then branch ij is in operation at stage y , whereas if
 235 both are equal to 0, then branch ij is out of operation at that stage. Furthermore, the direction of
 236 the flow across a particular branch ij at a given stage y is also modeled by the values of variables
 237 $w_{ij,y}^{B+}$ and $w_{ij,y}^{B-}$. Thus, the combination $w_{ij,y}^{B+} = 1$ and $w_{ij,y}^{B-} = 0$ is used to identify that node i is
 238 upstream of node j and, hence, the flow is from i to j . Conversely, the combination $w_{ij,y}^{B+} = 0$ and
 239 $w_{ij,y}^{B-} = 1$ is used to identify that node i is downstream of node j and, hence, the flow is from j to
 240 i . Expressions (19) ensure that fixed branches solely use the original conductor type.

241 According to (20), the planner can only invest once at most in each substation. Similarly, ex-
 242 pressions (21) impose a maximum of one new transformer installation per substation throughout
 243 the planning horizon. As per (22), the installation of new transformers happens after the corre-

244 sponding substation investment. Expressions (23) guarantee that new transformers operate only if
 245 the related investment has already been made. Moreover, constraints (24) ensure the use of one
 246 new transformer type at most for each substation at each stage of the planning horizon. Lastly, the
 247 binary nature of investment and operational variables is set in (25)–(30).

248 3.3. Effect of the Distribution Network

249 Expressions (31)–(41) represent the ac power flow model for a radially operated distribution
 250 network based on the set of recursive equations proposed in [34]:

$$\sum_{ki \in \mathcal{B}} \sum_{c \in \mathcal{C}} P_{ki,c,l,y} - \sum_{ij \in \mathcal{B}} \sum_{c \in \mathcal{C}} \left(P_{ij,c,l,y} + R_c \ell_{ij} I_{ij,c,l,y}^{sqr} \right) + P_{i,l,y}^{Sh} + P_{i,l,y}^S = F_l^D P_{i,y}^D; \quad (31)$$

$\forall i \in \mathcal{N}, \forall l \in \mathcal{L}, \forall y \in \mathcal{Y}$

$$\sum_{ki \in \mathcal{B}} \sum_{c \in \mathcal{C}} Q_{ki,c,l,y} - \sum_{ij \in \mathcal{B}} \sum_{c \in \mathcal{C}} \left(Q_{ij,c,l,y} + X_c \ell_{ij} I_{ij,c,l,y}^{sqr} \right) + Q_{i,l,y}^{Sh} + Q_{i,l,y}^S + Q_{i,l,y}^{CB} = F_l^D Q_{i,y}^D; \quad (32)$$

$\forall i \in \mathcal{N}, \forall l \in \mathcal{L}, \forall y \in \mathcal{Y}$

$$V_{i,l,y}^{sqr} = V_{j,l,y}^{sqr} + \sum_{c \in \mathcal{C}} [2(R_c P_{ij,c,l,y} + X_c Q_{ij,c,l,y}) \ell_{ij} - Z_c^2 \ell_{ij}^2 I_{ij,c,l,y}^{sqr}] + \Delta_{ij,l,y}^V; \quad (33)$$

$\forall ij \in \mathcal{B}, \forall l \in \mathcal{L}, \forall y \in \mathcal{Y}$

$$-\bar{\Delta}^V \left[1 - \left(w_{ij,y}^{B+} + w_{ij,y}^{B-} \right) \right] \leq \Delta_{ij,l,y}^V \leq \bar{\Delta}^V \left[1 - \left(w_{ij,y}^{B+} + w_{ij,y}^{B-} \right) \right]; \quad (34)$$

$\forall ij \in \mathcal{B}, \forall l \in \mathcal{L}, \forall y \in \mathcal{Y}$

$$V_{j,l,y}^{sqr} \hat{I}_{ij,l,y}^{sqr} = \hat{P}_{ij,l,y}^2 + \hat{Q}_{ij,l,y}^2; \forall ij \in \mathcal{B}, \forall l \in \mathcal{L}, \forall y \in \mathcal{Y} \quad (35)$$

$$\hat{I}_{ij,l,y}^{sqr} = \sum_{c \in \mathcal{C}} I_{ij,c,l,y}^{sqr}; \forall ij \in \mathcal{B}, \forall l \in \mathcal{L}, \forall y \in \mathcal{Y} \quad (36)$$

$$\hat{P}_{ij,l,y} = \sum_{c \in \mathcal{C}} P_{ij,c,l,y}; \forall ij \in \mathcal{B}, \forall l \in \mathcal{L}, \forall y \in \mathcal{Y} \quad (37)$$

$$\hat{Q}_{ij,l,y} = \sum_{c \in \mathcal{C}} Q_{ij,c,l,y}; \forall ij \in \mathcal{B}, \forall l \in \mathcal{L}, \forall y \in \mathcal{Y} \quad (38)$$

$$P_{i,l,y}^{Sh} \leq F_l^D P_{i,y}^D; \forall i \in \mathcal{N}, \forall l \in \mathcal{L}, \forall y \in \mathcal{Y} \quad (39)$$

$$Q_{i,l,y}^{Sh} = \tan(\cos^{-1}(pfi)) P_{i,l,y}^{Sh}; \forall i \in \mathcal{N}, \forall l \in \mathcal{L}, \forall y \in \mathcal{Y} \quad (40)$$

$$S_{i,l,y}^{S,sqr} \geq (P_{i,l,y}^S)^2 + (Q_{i,l,y}^S)^2; \forall i \in \mathcal{SN}, \forall l \in \mathcal{L}, \forall y \in \mathcal{Y} \quad (41)$$

251 where $V_{i,l,y}^{sqr}$ and $I_{ij,c,l,y}^{sqr}$ represent $V_{i,l,y}^2$ and $I_{ij,c,l,y}^2$, respectively.

252 Expressions (31) and (32) respectively ensure the active and reactive power balances at each
 253 node, i.e., Kirchhoff's first law, while accounting for network losses. Expressions (33) and (34) cor-
 254 respond to Kirchhoff's second law. Expressions (33) model branch voltage drops through auxiliary
 255 variables $\Delta_{ij,l,y}^V$, which are bounded in (34). As per (34), $\Delta_{ij,l,y}^V$ is equal to 0 for those branches ij
 256 in operation at stage y , for which $w_{ij,y}^{B+} + w_{ij,y}^{B-}$ is equal to 1. Thus, $\Delta_{ij,l,y}^V$ has no effect on (33), as
 257 desired. Conversely, for unused branches ij at stage y , for which $w_{ij,y}^{B+} + w_{ij,y}^{B-}$ is equal to 0, $\Delta_{ij,l,y}^V$
 258 lies in the interval $[-\bar{\Delta}^V, \bar{\Delta}^V]$. Hence, a sufficiently large value for $\bar{\Delta}^V$ ensures the deactivation of
 259 (33), as desired. Expressions (35) establish the relationship between active and reactive power flows
 260 $\hat{P}_{ij,l,y}$ and $\hat{Q}_{ij,l,y}$, squared current magnitudes $\hat{I}_{ij,l,y}^{sqr}$, and squared voltage magnitudes $V_{j,l,y}^{sqr}$. $\hat{I}_{ij,l,y}^{sqr}$,
 261 $\hat{P}_{ij,l,y}$, and $\hat{Q}_{ij,l,y}$ are respectively defined in (36)–(38), which rely on the fact that each branch uses
 262 a single conductor type at each planning stage. Additionally, nodal load shedding is limited as per

263 (39) and (40), whereas the active, reactive, and apparent power injections at substation nodes are
 264 related by (41).

Note that (35) and (41) contain nonlinear terms that can be linearized as described in [24].
 Based on the limited range within which nodal voltage magnitudes lie in practice, the product
 $V_{j,l,y}^{sqr} \hat{I}_{ij,l,y}^{sqr}$ in (35) can be linearized as follows:

$$V_{j,l,y}^{sqr} \hat{I}_{ij,l,y}^{sqr} \approx V_{j,l,y}^{est} \hat{I}_{ij,l,y}^{sqr}; \forall ij \in \mathcal{B}, \forall l \in \mathcal{L}, \forall y \in \mathcal{Y} \quad (42)$$

265 where parameters $V_{j,l,y}^{est}$ are estimated squared voltage magnitudes.

266 Analogously, the quadratic terms in the right-hand sides of (35) and (41) can be linearized using
 267 a piecewise approximation, as described in Appendix B.

268 Expressions (31)–(34), (36)–(40), and the linearized versions of (35) and (41) are essential pillars
 269 of the modeling contribution featured by this paper. The significant departure from closely related
 270 non-simulation-based models [19–23] comprises the capability to consider different power factors
 271 across the system, unlike [19–21], while overcoming the limitation of [22, 23], namely the absence
 272 of network losses and current limits.

273 3.4. Operational Limits

274 Expressions (43)–(48) set the acceptable ranges of the operational variables taking into account
 275 the investment decisions and operational statuses of branches and substations:

$$\underline{V}^2 \leq V_{i,l,y}^{sqr} \leq \bar{V}^2; \forall i \in \mathcal{N}, \forall l \in \mathcal{L}, \forall y \in \mathcal{Y} \quad (43)$$

$$0 \leq I_{ij,c,l,y}^{sqr} \leq \bar{I}_c^2 w_{ij,c,y}^B; \forall ij \in \mathcal{B}, \forall c \in \mathcal{C}, \forall l \in \mathcal{L}, \forall y \in \mathcal{Y} \quad (44)$$

$$-\bar{S}_{ij,c}^B w_{ij,c,y}^B \leq P_{ij,c,l,y} \leq \bar{S}_{ij,c}^B w_{ij,c,y}^B; \forall ij \in \mathcal{B}, \forall c \in \mathcal{C}, \forall l \in \mathcal{L}, \forall y \in \mathcal{Y} \quad (45)$$

$$-\bar{S}_{ij,c}^B w_{ij,c,y}^B \leq Q_{ij,c,l,y} \leq \bar{S}_{ij,c}^B w_{ij,c,y}^B; \forall ij \in \mathcal{B}, \forall c \in \mathcal{C}, \forall l \in \mathcal{L}, \forall y \in \mathcal{Y} \quad (46)$$

$$0 \leq Q_{i,l,y}^{CB} \leq \bar{Q}_i^{CB}; \forall i \in \mathcal{N}, \forall l \in \mathcal{L}, \forall y \in \mathcal{Y} \quad (47)$$

$$S_{i,l,y}^{S,sqr} \leq (\bar{S}_i^{S,ex} w_{i,y}^{S,ex} + \sum_{t \in \mathcal{T}} \bar{S}_t^T w_{i,t,y}^T)^2; \forall i \in \mathcal{SN}, \forall l \in \mathcal{L}, \forall y \in \mathcal{Y}. \quad (48)$$

276 The above expressions represent the limits for voltages (43), currents (44), active power flows
 277 (45), reactive power flows (46), reactive power injections of capacitor banks (47), and levels of
 278 apparent power injected by substations (48).

279 Nonlinear expressions (48) can be cast in a linear way as follows. First, the right-hand-side term
 280 is expanded:

$$\begin{aligned} S_{i,l,y}^{S,sqr} \leq & \left(\bar{S}_i^{S,ex} w_{i,y}^{S,ex} \right)^2 + \left(\bar{S}_1^T w_{i,1,y}^T \right)^2 + \dots + \left(\bar{S}_{|\mathcal{T}|}^T w_{i,|\mathcal{T}|,y}^T \right)^2 + 2 \left(\bar{S}_i^{S,ex} w_{i,y}^{S,ex} \right) \left(\bar{S}_1^T w_{i,1,y}^T \right) + \dots + \\ & 2 \left(\bar{S}_i^{S,ex} w_{i,y}^{S,ex} \right) \left(\bar{S}_{|\mathcal{T}|}^T w_{i,|\mathcal{T}|,y}^T \right) + 2 \left(\bar{S}_1^T w_{i,1,y}^T \right) \left(\bar{S}_2^T w_{i,2,y}^T \right) + \dots + 2 \left(\bar{S}_1^T w_{i,1,y}^T \right) \left(\bar{S}_{|\mathcal{T}|}^T w_{i,|\mathcal{T}|,y}^T \right) + \dots + \\ & 2 \left(\bar{S}_{|\mathcal{T}|-1}^T w_{i,|\mathcal{T}|-1,y}^T \right) \left(\bar{S}_{|\mathcal{T}|}^T w_{i,|\mathcal{T}|,y}^T \right); \forall i \in \mathcal{SN}, \forall l \in \mathcal{L}, \forall y \in \mathcal{Y}. \end{aligned} \quad (49)$$

281 The terms in the right-hand side of (49) involve products of binary variables $w_{i,y}^{S,ex}$ and $w_{i,t,y}^T$,
 282 which are subsequently linearized as described in Appendix B.

283 3.5. Radiality Constraints

284 In [25], a set of constraints was presented to guarantee the radial operation for the reconfiguration
 285 problem of distribution systems. Expressions (50)–(52) together with (18) extend that model for
 286 the radially operated meshed distribution networks considered in the planning problem at hand:

$$\sum_{ji \in \mathcal{B}} w_{ji,y}^{B+} + \sum_{ij \in \mathcal{B}} w_{ij,y}^{B-} = 0; \forall i \in \mathcal{SN}, \forall y \in \mathcal{Y} \quad (50)$$

$$\sum_{ji \in \mathcal{B}} w_{ji,y}^{B+} + \sum_{ij \in \mathcal{B}} w_{ij,y}^{B-} = 1; \forall i \in \mathcal{N} \setminus \mathcal{SN}, \forall y \in \mathcal{Y} | P_{i,y}^D > 0 \quad (51)$$

$$\sum_{ji \in \mathcal{B}} w_{ji,y}^{B+} + \sum_{ij \in \mathcal{B}} w_{ij,y}^{B-} \leq 1; \forall i \in \mathcal{N} \setminus \mathcal{SN}, \forall y \in \mathcal{Y} | P_{i,y}^D = 0. \quad (52)$$

287 Expressions (50) ensure that, for those branches connecting load nodes to substations, the
 288 substation node is the sending node. Expressions (51) guarantee that each load node is the receiving
 289 node of a single branch. Finally, transfer nodes, i.e., nodes without demand that are used to connect
 290 two load nodes, are modeled in (52).

291 It is worth emphasizing that the proposed radiality constraints (50)–(52), which are suitable for
 292 an unknown network topology, extend those presented in [25] for a given grid layout. Such a nontrivial
 293 extension constitutes a relevant part of the first contribution listed in Section 1 as it represents
 294 a salient modeling feature over the state-of-the-art radiality constraints used in distribution system
 295 planning [35]. Note that, unlike [35], neither auxiliary variables nor fictitious flows are required,
 296 thereby leading to a more efficient equivalent model from a computational perspective. Moreover,
 297 the proposed radiality model substantially differs from those used in closely related formulations for
 298 multistage reliability-constrained distribution network expansion planning [19–21], which rely on a
 299 single binary variable for branch operation, and [23], where radial operation under the normal state
 300 and transfer nodes are both disregarded.

301 3.6. Reliability Constraints

302 This section is devoted to modeling the effect of branch outages on EENS. To that end, the
 303 expected durations of both repair-and-switching and switching-only nodal interruptions, $\Gamma_{i,y}^{RS}$ and
 304 $\Gamma_{i,y}^{SO}$, which are required to determine $EENS_y$ as per (7), are formulated in terms of branch failure
 305 rates, λ_{ij} , and branch interruption durations, τ_{ij}^{RS} and τ_{ij}^{SO} .

306 In [15], linear algebra was proposed to model standard reliability indices for a radial system.
 307 As a major computational advantage, such a reliability assessment algebraic model overcomes the
 308 dimensionality issue of the non-simulation-based approaches reported in [14] and [17, 18] and ap-
 309 plied in [19] and [22, 23], respectively. Here, we propose leveraging the findings of [15] to explicitly
 310 incorporate reliability in the mathematical formulation of multistage reliability-constrained distri-
 311 bution network expansion planning. It is worth mentioning that the proposed reliability model
 312 features a major distinctive aspect over the formulation of [15], namely the capability of handling
 313 the lack of knowledge of the network topology along the planning horizon, which is an outcome of
 314 the optimization process. The proposed reliability constraints are formulated as follows:

$$\Gamma_{i,y}^{RS} = \Gamma_{j,y}^{RS} + \tau_{ij}^{RS} \lambda_{ij} \ell_{ij} w_{ij,y}^{B-} - \tau_{ij}^{RS} \lambda_{ij} \ell_{ij} w_{ij,y}^{B+} + \Delta_{ij,y}^{RS}; \forall ij \in \mathcal{B}, \forall y \in \mathcal{Y} \quad (53)$$

$$- \bar{\Delta}^{RS} \left[1 - \left(w_{ij,y}^{B+} + w_{ij,y}^{B-} \right) \right] \leq \Delta_{ij,y}^{RS} \leq \bar{\Delta}^{RS} \left[1 - \left(w_{ij,y}^{B+} + w_{ij,y}^{B-} \right) \right]; \forall ij \in \mathcal{B}, \forall y \in \mathcal{Y} \quad (54)$$

$$\Gamma_{i,y}^{SO} = \Gamma_{j,y}^{SO} - \tau_{ij}^{SO} \lambda_{ij} \ell_{ij} w_{ij,y}^{B-} + \tau_{ij}^{SO} \lambda_{ij} \ell_{ij} w_{ij,y}^{B+} + \Delta_{ij,y}^{SO}; \forall ij \in \mathcal{B} | i, j \notin \mathcal{SN}, \forall y \in \mathcal{Y} \quad (55)$$

$$- \bar{\Delta}^{SO} \left[1 - \left(w_{ij,y}^{B+} + w_{ij,y}^{B-} \right) \right] \leq \Delta_{ij,y}^{SO} \leq \bar{\Delta}^{SO} \left[1 - \left(w_{ij,y}^{B+} + w_{ij,y}^{B-} \right) \right];$$

$$\forall ij \in \mathcal{B} | i, j \notin \mathcal{SN}, \forall y \in \mathcal{Y} \quad (56)$$

$$\sum_{\substack{ji \in \mathcal{B} \\ j \notin \mathcal{SN}}} f_{ji,y}^{SO} - \sum_{\substack{ij \in \mathcal{B} \\ j \notin \mathcal{SN}}} f_{ij,y}^{SO} + \Psi_{i,y}^{SO} = \sum_{\substack{ji \in \mathcal{B} \\ j \notin \mathcal{SN}}} \tau_{ji}^{SO} \lambda_{ji} \ell_{ji} w_{ji,y}^{B+} + \sum_{\substack{ij \in \mathcal{B} \\ j \notin \mathcal{SN}}} \tau_{ij}^{SO} \lambda_{ij} \ell_{ij} w_{ij,y}^{B-};$$

$$\forall i \in \mathcal{RN}, \forall y \in \mathcal{Y} \quad (57)$$

$$\sum_{\substack{ji \in \mathcal{B} \\ j \notin \mathcal{SN}}} f_{ji,y}^{SO} - \sum_{\substack{ij \in \mathcal{B} \\ j \notin \mathcal{SN}}} f_{ij,y}^{SO} = \sum_{\substack{ji \in \mathcal{B} \\ j \notin \mathcal{SN}}} \tau_{ji}^{SO} \lambda_{ji} \ell_{ji} w_{ji,y}^{B+} + \sum_{\substack{ij \in \mathcal{B} \\ j \notin \mathcal{SN}}} \tau_{ij}^{SO} \lambda_{ij} \ell_{ij} w_{ij,y}^{B-};$$

$$\forall i \in \mathcal{N} \setminus \mathcal{RN}, \forall y \in \mathcal{Y} \quad (58)$$

$$-\bar{\Delta}^{SO} \left(w_{ij,y}^{B+} + w_{ij,y}^{B-} \right) \leq f_{ij,y}^{SO} \leq \bar{\Delta}^{SO} \left(w_{ij,y}^{B+} + w_{ij,y}^{B-} \right); \forall ij \in \mathcal{B} | i, j \notin \mathcal{SN}, \forall y \in \mathcal{Y} \quad (59)$$

$$0 \leq \Psi_{i,y}^{SO} \leq \bar{\Delta}^{SO} \left(w_{ij,y}^{B+} + w_{ij,y}^{B-} \right); \forall ij \in \mathcal{B} | j \in \mathcal{SN}, \forall y \in \mathcal{Y} \quad (60)$$

$$0 \leq \Psi_{j,y}^{SO} \leq \bar{\Delta}^{SO} \left(w_{ij,y}^{B+} + w_{ij,y}^{B-} \right); \forall ij \in \mathcal{B} | i \in \mathcal{SN}, \forall y \in \mathcal{Y} \quad (61)$$

$$\Gamma_{i,y}^{SO} \geq \Psi_{i,y}^{SO}; \forall i \in \mathcal{RN}, \forall y \in \mathcal{Y} \quad (62)$$

$$\Gamma_{i,y}^{RS} = 0; \forall i \in \mathcal{SN}, \forall y \in \mathcal{Y} \quad (63)$$

$$\Gamma_{i,y}^{SO} = 0; \forall i \in \mathcal{SN}, \forall y \in \mathcal{Y} \quad (64)$$

$$\Gamma_{i,y}^{SO} \geq 0; \forall i \in \mathcal{N}, \forall y \in \mathcal{Y} \quad (65)$$

$$\Gamma_{i,y}^{RS} \geq 0; \forall i \in \mathcal{N}, \forall y \in \mathcal{Y}. \quad (66)$$

315 The calculation of nodal reliability indices in distribution networks requires modeling the direc-
 316 tion of branch flows. Here, this topological information is directly provided by variables $w_{ij,y}^{B+}$ and
 317 $w_{ij,y}^{B-}$ as described in Section 3.2. Note that, unlike [19], the use of variables $w_{ij,y}^{B+}$ and $w_{ij,y}^{B-}$ precludes
 318 the need for additional topology-dependent variables.

319 Expressions (53) and (54) model the expected durations of repair-and-switching interruptions
 320 affecting load nodes. If the flow at stage y is from i to j , i.e., $w_{ij,y}^{B+} = 1$ and $w_{ij,y}^{B-} = 0$, then
 321 expressions (53) become $\Gamma_{i,y}^{RS} = \Gamma_{j,y}^{RS} - \tau_{ij}^{RS} \lambda_{ij} \ell_{ij}$, as desired. Note that $\Delta_{ij,y}^{RS}$ is equal to 0 as per
 322 (54). On the other hand, if the flow at stage y is from j to i , i.e., $w_{ij,y}^{B+} = 0$ and $w_{ij,y}^{B-} = 1$, then
 323 expressions (53) become $\Gamma_{i,y}^{RS} = \Gamma_{j,y}^{RS} + \tau_{ij}^{RS} \lambda_{ij} \ell_{ij}$. This desired result stems from the fact that $\Delta_{ij,y}^{RS}$
 324 is equal to 0 according to (54). When branch ij is not in operation at stage y , i.e., $w_{ij,y}^{B+} = w_{ij,y}^{B-} = 0$,
 325 expressions (53) are relaxed as $\Delta_{ij,y}^{RS}$ may vary freely within a sufficiently large range as modeled in
 326 (54) for a suitable value of parameter $\bar{\Delta}^{RS}$.

327 Expressions (55) and (56) characterize the expected durations of switching-only interruptions
 328 affecting load nodes. Similar to (53)–(54) for repair-and-switching interruptions, variables $w_{ij,y}^{B+}$
 329 and $w_{ij,y}^{B-}$ and the bounding parameter $\bar{\Delta}^{SO}$ are used to compute the expected nodal durations of
 330 switching-only interruptions. Moreover, note that expressions (53)–(54) and (55)–(56) are respec-
 331 tively similar to the formulation for the branch voltage drops (33)–(34).

332 Expressions (57)–(62) allow modeling the expected duration of switching-only interruptions of
 333 every root node, which is equal to the sum of the durations of switching-only interruptions of all
 334 branches downstream [15]. Based on the findings of [15] for a given radial topology, expressions
 335 (57)–(62) represent the operation, i.e., the load flow, under a special loading condition of a particular
 336 fictitious lossless system with an *a priori* unknown topology. According to [15], such a load flow
 337 allows characterizing via optimization variables the topological information required to compute the
 338 standard reliability index considered in this paper, namely the expected energy not supplied.

339 Fig. 1 is useful to gain insight into how expressions (57)–(62) work. Fig. 1(a) shows the system
 340 used for illustration purposes. The original system comprises eight load nodes represented by circles,
 341 one existing substation depicted as a solid square, one candidate substation plotted as a dashed
 342 square, five existing branches indicated by solid lines, and seven candidate branches represented by
 343 dashed lines. The fictitious system is obtained from the original system by removing all substation
 344 nodes and the branches (existing and candidate) that connect them to the root nodes. Consequently,

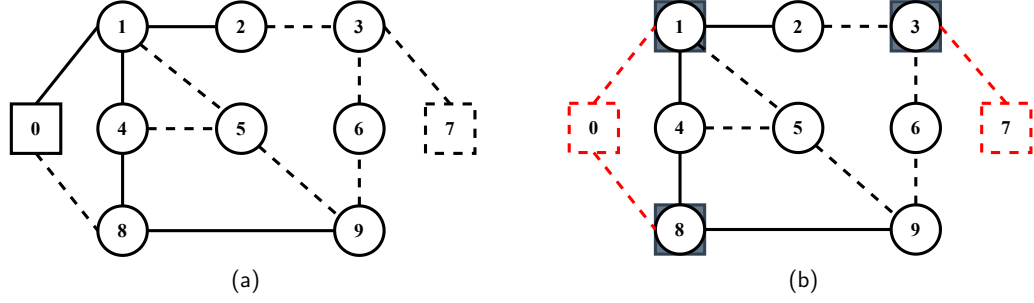


Figure 1: Illustrative example. (a) Original system. (b) Fictitious system.

345 the root nodes in the original system are potential source nodes in the fictitious system. To play
 346 such a role in the fictitious system, the root nodes in the original system must be connected to
 347 a substation by an operating branch, which is modeled by $w_{ij,y}^{B+} = 1$ with i indexing a substation
 348 node, or by $w_{ij,y}^{B-} = 1$ with j indexing a substation node. In addition, all branches connecting
 349 the nodes in the fictitious system are respectively identical to the corresponding branches (existing
 350 and candidate) in the original system. The fictitious system associated with the original system
 351 represented in Fig. 1(a) is shown in Fig. 1(b), where the removed assets are highlighted using dotted
 352 red lines and the original root nodes are inside a square to indicate their role as potential source
 353 nodes in the fictitious system.

354 The following nodal demands characterize the special loading condition for the fictitious system.
 355 Demands at fictitious source nodes are all zero. Fictitious demand nodes comprise original load
 356 nodes together with the root nodes without connection to any substation. The demand at each of
 357 these fictitious nodes is equal to the product of the failure rate and the switching-only interruption
 358 duration of the only operating branch that connects this node to the upstream node.

359 Bearing in mind that 1) the fictitious system is lossless, topologically similar to the original
 360 network, and radially operated, 2) the sources of this fictitious system are located at the root nodes
 361 of the original system, and 3) the non-zero-valued demands of the special loading condition are equal
 362 to the products of failure rates and switching-only interruption durations, the expected durations of
 363 switching-only interruptions for the root nodes becoming sources of the fictitious system are equal
 364 to the corresponding generation levels resulting from the load flow solution. Further details on the
 365 underlying rationale for (57)–(62) can be found in [15].

366 In (57)–(62), branch power flows in the fictitious system are modeled by variables $f_{ij,y}^{SO}$, which
 367 depend on $w_{ij,y}^{B+}$ and $w_{ij,y}^{B-}$ (59). Expressions (57) model the power balance for the root nodes. If root
 368 node i becomes a source node in the fictitious system at stage y , i.e., there is at least one branch ij
 369 in operation such that j indexes a substation node, expressions (60)–(61) allow fictitious generation
 370 to be injected at node i , which is modeled by variables $\Psi_{i,y}^{SO}$. Consequently, as per (51), the other
 371 branches feeding root node i are not operating at stage y , i.e., $\sum_{ji \in \mathcal{B}|j \notin \mathcal{SN}} w_{ji,y}^{B+} + \sum_{ij \in \mathcal{B}|j \notin \mathcal{SN}} w_{ij,y}^{B+} = 0$,

372 and, thus, the right-hand side of (57) is equal to 0. Conversely, if root node i is not connected
 373 to any substation of the original system by a branch in operation at stage y , i.e., $w_{ij,y}^{B+} + w_{ij,y}^{B-} =$
 374 $0, \forall ij \in \mathcal{B}|j \in \mathcal{SN}$, then $\Psi_{i,y}^{SO} = 0$ as set in (60)–(61). Hence, according to (51), another branch is
 375 operating at stage y to feed root node i , i.e., $\sum_{ji \in \mathcal{B}|j \notin \mathcal{SN}} w_{ji,y}^{B+} + \sum_{ij \in \mathcal{B}|j \notin \mathcal{SN}} w_{ij,y}^{B+} = 1$. Moreover, the

376 right-hand side of (57) determines the fictitious demand for such a root node, which is equal to the
 377 product of the failure rate and the switching-only interruption duration of that branch in operation.

378 Expressions (58) represent the power balance for the load nodes of the original system excluding
 379 the root nodes. For a given load node, the right-hand side of (58) sets the demand equal to

380 the product of the failure rate and the switching-only interruption duration of the only branch in
 381 operation connecting this node to the upstream node.

382 Expressions (62) set the relationship between $\Gamma_{i,y}^{SO}$ and $\Psi_{i,y}^{SO}$ for the root nodes. Note that, for
 383 the root nodes that become source nodes of the fictitious system, the minimization of the objective
 384 function leads to $\Gamma_{i,y}^{SO} = \Psi_{i,y}^{SO}$. On the other hand, for the root nodes that are load nodes of the
 385 fictitious system, $\Gamma_{i,y}^{SO} \geq 0$. The standard values of the expected interruption durations at substation
 386 nodes are established in (63)–(64). Finally, the non-negativity of expected interruption durations
 387 is set in (65)–(66).

388 Overall, expressions (53)–(66) play a key role in terms of the modeling contribution of this
 389 paper as reliability is effectively incorporated into multistage distribution network expansion plan-
 390 ning without requiring the explicit characterization of system operation for every outage and while
 391 considering switching-only interruptions, which are the main limitations of state-of-the-art works
 392 [19, 22, 23] and [20, 21], respectively.

393 3.7. Mixed-Integer Linear Formulation

394 The proposed planning model is a mixed-integer nonlinear program that can be recast as an
 395 instance of mixed-integer linear programming. To that end, nonlinear expressions (35), (41), and
 396 (49) are replaced with linear terms using (42) and the linearization schemes described in Appendix
 397 B. For the sake of completeness, the resulting mixed-integer linear program is formulated as:

$$\begin{aligned} \text{Minimize } c^{PV} = & \sum_{y \in \mathcal{Y}} \frac{(1 + I_r)^{-y}}{I_r} c_y^I + \sum_{y \in \mathcal{Y}} \left[(1 + I_r)^{-y} \left(c_y^M + c_y^E + c_y^{Sh} + c_y^{ENS} \right) \right] + \\ & \frac{(1 + I_r)^{-|\mathcal{Y}|}}{I_r} \left(c_{|\mathcal{Y}|}^M + c_{|\mathcal{Y}|}^E + c_{|\mathcal{Y}|}^{Sh} + c_{|\mathcal{Y}|}^{ENS} \right) \end{aligned} \quad (67)$$

subject to:

$$\text{Expressions (2)–(34), (36)–(40), (43)–(47), and (50)–(66)} \quad (68)$$

$$\text{Linearized versions of (35), (41), and (49).} \quad (69)$$

398 Problem (67)–(69) relies on the selection of appropriate values for bounding parameters $\overline{\Delta}^{RS}$,
 399 $\overline{\Delta}^{SO}$, and $\overline{\Delta}^V$. It should be noted that the tuning of such parameters benefits from two relevant
 400 aspects:
 401

- 402 1. No matter the system size and the number of stages, only three bounding parameters require
 403 adjustment.
- 404 2. Suitable practical values are readily available for the three bounding parameters. Thus, $\overline{\Delta}^{RS}$
 405 can be set equal to the sum over all branches in the network of the products of the corre-
 406 sponding repair-and-switching interruption duration and failure rate. Similarly, $\overline{\Delta}^{SO}$ can be
 407 set equal to the sum over all branches in the network of the products of the corresponding
 408 switching-only interruption duration and failure rate. Finally, $\overline{\Delta}^V$ can be set equal to the
 409 difference between the upper and lower voltage limits of the network under planning.

410 Moreover, as tighter values for $\overline{\Delta}^{RS}$, $\overline{\Delta}^{SO}$, and $\overline{\Delta}^V$ may be advantageous from a computational
 411 perspective, using as initial values those mentioned in the above item 2, we have implemented
 412 a trial-and-error selection procedure relying on the stabilization of the resulting investment plan
 413 whereby the values of such parameters are iteratively tightened.

414 The use of mixed-integer linear programming in problem (67)–(69) to effectively address multi-
 415 stage reliability-constrained distribution network expansion planning represents the methodological
 416 contribution of this paper as finite convergence to optimality is guaranteed and a measure of the
 417 distance to optimality is provided. Moreover, problem (67)–(69) is suitable for off-the-shelf soft-
 418 ware based on the state-of-the-art branch-and-cut algorithm [29], which is beneficial for practical
 419 implementation purposes.

420 4. Numerical Results

421 The proposed model has been applied to the 54-node test system addressed in [19] consider-
 422 ing a 10-year planning horizon, a \$2-million investment budget, and a 15-block piecewise linear
 423 approximation for the ac power flow. Based on [19, 27], the cost coefficient for EENS, C^{EENS} , is
 424 \$11200/MWh. Due to space limitations, a complete description of the case study, including all
 425 system parameters, is available in [36], thereby enabling full reproducibility and a comprehensive
 426 analysis of results.

427 For assessment purposes, we have implemented the formulation presented in [19] and a modified
 428 version of the model described in [23]. Note that both references represent the state of the art for
 429 the exact incorporation of reliability into the multistage distribution network expansion planning
 430 problem. In the first benchmark, 1) an alternative albeit significantly larger reliability constraint set
 431 is considered, and 2) reactive power is not explicitly modeled as a constant power factor is assumed.
 432 As for the second benchmark, major modifications to the formulation presented in [23] include 1) the
 433 replacement of the objective function with that considered in our formulation, 2) the extension of
 434 the model to consider different load levels and radial operation under normal conditions, as, unlike in
 435 our approach, both aspects are disregarded in [23], and 3) the removal of the constraints associated
 436 with infrastructure aging, as such a modeling aspect is neglected in our formulation. Simulations
 437 have been run on a Dell PowerEdge R920X64 with four Intel[®] Xeon[®] E7-4820 processors at 2.00
 438 GHz and 768 GB of RAM using GAMS 24.7 and CPLEX 12.6 [37]. For all models, the optimality
 439 tolerance of CPLEX was set at 0%.

440 Table 2 reports the investment plans attained for the three models, the corresponding investment
 441 topologies being available in [36]. It should be noted that the simulations of both the proposed
 442 approach and the benchmark relying on [19] were successfully run to optimality. Unfortunately, for
 443 the model based on [23], the solver was unable to reduce the optimality gap under 99.07% after one
 444 week. This result reveals the computational impact of considering both a yearly discretization of
 445 the planning horizon and the practical aspects disregarded in [23] such as radial operation under
 446 the normal state and the chronological aspect of demand for network operation.

447 In Table 2, single figures designate nodes, pairs of figures connected by a hyphen indicate
 448 branches, whereas Ak , Rk , and Tk respectively denote the installation of alternative k for a branch
 449 subject to addition, for a branch subject to replacement, and for a candidate transformer. As can
 450 be observed, the expansion plans for the proposed model and the benchmark based on [19] mainly
 451 differ in 9 branches, namely 3-4, 3-51, 8-25, 16-40, 33-39, and 42-47, which are installed according to
 452 the proposed model, and 24-25, 38-39, and 46-47, which are built as per the benchmark. Additional
 453 significant differences are featured in 1) the alternatives installed in the substations at nodes 51,
 454 52, and 54, and in branch 35-36, and 2) the installation times of branches 1-9, 11-52, 12-45, 33-34,
 455 34-35, 35-36, 38-45, and 44-45. Analogously, Table 2 also shows that the solutions identified for
 456 the proposed approach and the benchmark based on [23] are significantly different regarding 1) the
 457 installation of new substations and branches, 2) the use of investment and replacement alternatives,
 458 and 3) the timing of expansion decisions. Such substantial disparities motivate the need for the
 459 proposed approach.

Table 2: Investment Plans

Stage	Proposed model		Benchmark [19]		Benchmark [23]	
1	9-17(A1)	30-43(A1)	9-17(A1)	30-43(A1)	17-18(A2)	
	10-31(A1)	30-54(A2)	10-31(A1)	30-54(A2)	18-19(A1)	
	18-19(A1)	31-37(A1)	18-19(A1)	31-37(A1)	19-20(A1)	
	18-21(A1)	37-43(A1)	18-21(A1)	37-43(A1)		
	21-54(A1)	54(T2)	21-54(A1)	54(T1)		
2	19-20(A1)		19-20(A1)		9-17(A1)	18-21(A2)
	22-54(A1)		22-54(A1)		9-22(A1)	
3	1-51(R2)	23-24(A1)	1-9(R1)	24-25(A1)	8-25(A1)	
	3-51(R1)	51(T2)	1-51(R2)	51(T1)	23-24(A1)	
	8-25(A1)		23-24(A1)			
4	26-27(A1)	28-53(A1)	26-27(A1)	28-53(A1)	8-27(A2)	28-53(A2)
	27-28(A1)	53(T2)	27-28(A1)	53(T2)	26-27(A1)	
5	29-30(A1)	34-35(A1)	12-45(A1)	38-44(A1)	10-31(A2)	
	32-39(A1)	35-36(A2)	29-30(A1)	44-45(A1)	29-30(A1)	
	33-34(A1)	36-53(A2)	32-39(A1)		30-54(A2)	
	33-39(A1)		38-39(A1)		32-39(A1)	
6			33-34(A1)	35-36(A1)	8-33(A1)	34-35(A2)
			34-35(A1)	36-53(A2)	33-34(A2)	35-36(A2)
7	12-45(A1)	44-45(A1)			31-37(A2)	37-43(A2)
	38-44(A1)				33-39(A1)	38-39(A2)
8	40-41(A1)	41-53(A1)	11-52(R1)	41-42(A1)	13-43(A2)	41-53(A1)
	41-42(A1)		40-41(A1)	41-53(A1)	40-41(A1)	42-48(A1)
9	3-4(R1)	16-40(A1)	14-46(A1)		12-45(A2)	44-45(A1)
	11-52(R1)	42-47(A1)	14-52(R2)		14-46(A1)	
	14-46(A1)	52(T1)	46-47(A1)		16-40(A2)	
	14-52(R2)		52(T2)		42-47(A1)	
10	1-9(R1)	48-49(A1)	14-50(A1)	49-50(A1)	14-50(A1)	49-50(A1)
	14-50(A1)	49-50(A1)	48-49(A1)		46-47(A1)	

Table 3: Present Values of Costs (10^3 \$)

	Proposed model	Benchmark [19]		Benchmark [23]	
		Approximate results	Actual results	Approximate results	Actual results
Investment	4,268.40	3,811.50	3,811.50	557.43	–
Production	134,026.01	135,044.60	134,032.57	68,307.72	–
Maintenance	281.51	279.23	279.23	190.46	–
Load shedding	0.00	0.00	26,797.48	12,063,895.10	–
Reliability	33,805.13	33,195.86	33,275.00	367,042.50	–
Total	172,381.05	172,331.19	198,195.78	12,499,993.21	–

460 Table 3 presents the economic results associated with the investment plans shown in Table 2.
461 The columns labeled as “Approximate results” list the costs provided by the models based on [19]
462 and [23], respectively. It is worth emphasizing that the operational costs, and, hence, the total cost,
463 reported in such columns are optimistic due to the use of either an approximate network model that
464 does not properly consider reactive power or a potentially infeasible reliability model neglecting the
465 effect of transfer nodes. Thus, for the sake of a fair comparison, we have computed the costs
466 resulting from solving the proposed model with expansion decisions fixed to those featured by the
467 investment plans identified by the benchmarks. Such actual costs are displayed in the columns of
468 Table 3 labeled as “Actual results”.

469 As can be seen in Table 3, the approximate operational costs characterizing the optimal solu-
470 tion to the benchmark based on [19] are very close to those associated with the optimal solution
471 to the proposed model. Moreover, according to the approximate network representation of the
472 benchmark, the resulting investment plan apparently complies with nodal power balance as the
473 cost of load shedding is null. However, the fourth column of Table 3 reveals that the operation
474 of the optimal investment plan resulting from the benchmark is far more expensive in reality and,
475 hence, a substantial 13.02% reduction in the total cost is attained by the proposed model. This
476 cost reduction is a consequence of the use of a more accurate characterization of the effect of the
477 distribution network. Note that the optimal investment plan for the benchmark, albeit giving rise
478 to a lower investment cost, actually fails to meet nodal power balance due to its reliance on an
479 approximate network model based on a constant power factor across the system. As a result, load
480 shedding is featured. By contrast, the proposed model yields an investment plan that does not
481 require load shedding, which offsets the investment cost increase.

482 Regarding the solution to the benchmark based on [23], the substantially larger values for load
483 shedding and reliability costs and the significantly lower investment cost reported in Table 3 indicate
484 that the resulting investment plan is far from optimal. More importantly, as can be seen in the last
485 column of this table, no actual results were reported for this poor-quality investment plan, which
486 led to infeasibility for the proposed model.

487 The suitability of the proposed linearized ac network model for multistage reliability-constrained
488 distribution network expansion planning has been further verified empirically. First, we have im-
489 plemented a modified version of the proposed planning model wherein the effect of the distribution
490 network is characterized by the formulation presented in [38], which is based on second-order cone
491 programming. Unfortunately, for this more accurate planning model, CPLEX failed to find a sin-
492 gle feasible solution after one week. In addition, we have used a full load flow model to quantify

Table 4: Reliability-Unconstrained Investment Plan

Stage	Investment decisions					
1	1-9(R2)	3-51(R2)	11-52(R2)	18-19(A1)	54(T2)	
	1-51(R2)	9-17(A1)	14-15(R2)	18-21(A1)		
	3-4(R2)	11-12(R2)	14-52(R2)	21-54(A1)		
2	19-20(A1)	22-54(A1)				
3	8-25(A1)	23-24(A1)	51(T2)			
4	26-27(A1)	27-28(A1)	28-53(A2)	53(T2)		
5	29-30(A1)	30-54(A2)	32-39(A1)	33-39(A1)	35-36(A2)	37-43(A1)
	30-43(A1)	31-37(A1)	33-34(A1)	34-35(A1)	36-53(A2)	
6						
7	12-45(A1)	38-44(A1)	44-45(A1)			
8	40-41(A1)	41-42(A1)	41-53(A1)			
9	52(T1)	14-46(A1)	16-40(A1)	46-47(A1)		
10	14-50(A1)	48-49(A1)	49-50(A1)			

the operational accuracy of the linearized network model. It is important to note that the load flow determines the system operation for all stages in a single run. The maximum absolute errors obtained for branch current flows, power injections at substations, and nodal voltage magnitudes were 0.39 A, 0.05 MVA, and 1.35 kV, respectively. The corresponding mean absolute errors were 0.04 A, 0.01 MVA, and 0.52 kV, with standard deviations equal to 0.06 A, 0.01 MVA, and 0.04 kV, respectively. Finally, the relative errors considering the total values of branch current flows, power injections at substations, and nodal voltage magnitudes amounted to 1.03%, 0.01%, and 0.31%, respectively. These results, which are consistent with those reported in [24], corroborate the relevant trade-off between tractability and modeling accuracy featured by the use of the proposed ac network formulation for planning purposes.

This case study is also useful to illustrate the computational benefits of the proposed algebraic formulation for reliability. To that end, we have run two modified versions of the proposed planning model wherein reliability constraints are replaced with those recently presented in [19] and [23], respectively. The proposed approach attained optimality in 14.53 h, whereas the modified model relying on [19] required 48.87 h, thereby increasing the computational burden by 3.36 times. As for the model based on the reliability formulation described in [23], the simulation failed again to identify a solution with acceptable quality. These results substantiate the computational superiority of the proposed model.

Finally, the impact of reliability has been examined by solving a reliability-unconstrained version of the proposed model wherein all reliability-related terms are dropped. The comparison of the resulting investment plan provided in Table 4 with that shown in Table 2 for the proposed model reveals that neglecting reliability yields the postponement of some branch investments, as is the case of branches 30-43, 30-54, 31-37, and 37-43, and the earlier implementation of several branch replacements, as is experienced by branches 3-4, 11-52, and 14-52.

The economic effect of the above changes in the investment plan are summarized in Table 5. In this table, column 2 lists the actual costs for the resulting expansion decisions should reliability be modeled, whereas ε in column 3 denotes the percent cost differences with respect to the results reported in Table 3 for the proposed approach. For this particular case study, disregarding reliability

Table 5: Economic Results for the Reliability-Unconstrained Investment Plan

Cost term	Present value (10^3 \$)	ε (%)
Investment	4,258.14	-0.24
Production	133,494.76	-0.40
Maintenance	300.34	6.69
Load shedding	0.00	–
Reliability	35,484.73	4.97
Total	173,537.97	0.67

521 yields slight reductions in the investment and production costs while moderately rising maintenance
 522 and reliability costs. Overall, the optimal expansion plan resulting from the reliability-unconstrained
 523 model is more expensive by \$1.16 million, which represents a 0.67% increase in the total cost.

524 5. Conclusion

525 This paper has presented a novel model for the multistage distribution network expansion plan-
 526 ning problem wherein reliability and radiality are explicitly formulated. The proposed approach
 527 features two relevant novelties. First, a novel and computationally efficient set of algebraic expres-
 528 sions is developed to explicitly incorporate a standard topology-dependent reliability metric, namely
 529 the expected energy not supplied, in the formulation of the planning problem. Second, both active
 530 and reactive power are precisely accounted for through an effective piecewise linear approximation of
 531 the ac power flow. As empirically evidenced, the resulting mixed-integer linear program outperforms
 532 the state-of-the-art models in terms of both solution quality and computational performance.

533 A. Nomenclature

534 The nomenclature used throughout this paper is provided below for quick reference.

Sets and Indices

\mathcal{B}	Set of indices ij, ji, ki of branch types. $\mathcal{B} = \mathcal{AB} \cup \mathcal{FB} \cup \mathcal{RB}$, where \mathcal{AB} , \mathcal{FB} , and \mathcal{RB} denote added branch, existing fixed branch, and existing replaceable branch, respectively.
\mathcal{C}	Set of indices c, e of conductor types.
\mathcal{L}	Set of indices l of load levels.
535 \mathcal{N}	Set of node indices i, j . $\mathcal{RN} \subseteq \mathcal{N}$, $\mathcal{SN} \subseteq \mathcal{N}$, where \mathcal{RN} and \mathcal{SN} are related to load nodes that may be directly connected to a substation (root nodes) and substation nodes, respectively.
\mathcal{T}	Set of indices t of transformer alternatives.
\mathcal{Y}	Set of indices p, y of yearly time stages.

Parameters

β^{FB}, β^{RB}	Initial conductor alternatives for existing fixed and replaceable branches.
Δ_l	Duration of load level l .
$\overline{\Delta}^{RS}, \overline{\Delta}^{SO}, \overline{\Delta}^V$	Upper bounds for the absolute value of $\Delta_{ij,y}^{RS}$, $\Delta_{ij,y}^{SO}$, and $\Delta_{ij,l,y}^V$.
η^B, η^S	Lifetimes of branches and substations.
λ_{ij}	Failure rate per unit length of branch ij .
$\tau_{ij}^{RS}, \tau_{ij}^{SO}$	Durations of the repair-and-switching and switching-only interruptions associated with the failure of branch ij .
φ_{ij}	Binary parameter that is equal to 1 if branch ij is switchable under normal operation, being 0 otherwise.
$C_{i,l}^E$	Cost coefficient for the energy supplied by the substation at node i and load level l .
C^{ENS}	Cost coefficient for the expected energy not supplied under branch outages.
$C_{ij,c}^{I,AB}, C_{ij,c}^{I,RB}$	Cost coefficients for the installation of conductor type c in added and replaceable branch ij .
$C_i^{I,S}, C_t^{I,T}$	Investment cost coefficients for substation installation at node i and for transformer alternative t .
$C_{ij,c}^{M,B}, C_i^{M,S}, C_t^{M,T}$	Maintenance cost coefficients for conductor type c for branch ij , for the substation at node i , and for transformer alternative t .
C^{Sh}	Cost coefficient for load shedding under normal operation.
F_l^D	Demand factor of load level l .
\bar{I}_c	Maximum current magnitude of conductor type c .
I_r	Interest rate.
l_{ij}	Length of branch ij .
$P_{i,y}^D, Q_{i,y}^D$	Active and reactive power peak demands at node i and stage y .
pf_i	Power factor at node i .
\overline{Q}_i^{CB}	Reactive power capacity of the capacitor bank at node i .
R_c, X_c, Z_c	Resistance, reactance, and impedance per unit length for conductor type c .
RR^B, RR^S	Capital recovery rates for investments in branches and substations.
$\overline{S}_{ij,c}^B$	Apparent power capacity of branch ij for conductor type c .
$\overline{S}_i^{S,ex}$	Original apparent power capacity of the existing substation at node i .
\overline{S}_t^T	Apparent power capacity of transformer alternative t .
$V_{i,l,y}^{est}$	Estimated squared voltage magnitude at node i , load level l , and stage y .

Continuous Variables

$\Delta_{ij,y}^{RS}, \Delta_{ij,y}^{SO}$	Auxiliary variables used to compute $\Gamma_{i,y}^{RS}$ and $\Gamma_{i,y}^{SO}$.
$\Delta_{ij,l,y}^V$	Squared voltage drop magnitude of branch ij for load level l and stage y .

	$\Gamma_{i,y}^{RS}, \Gamma_{i,y}^{SO}$	Expected durations of repair-and-switching and switching-only interruptions affecting node i at stage y .
	$\Psi_{i,y}^{SO}$	Generation supplied at node i of the fictitious system used at stage y to compute $\Gamma_{i,y}^{SO}$.
	$c_y^E, c_y^{ENS}, c_y^I,$ c_y^M, c_y^{Sh}	Costs of production, reliability, investment, maintenance, and load shedding at stage y .
	c^{PV}	Present value of the total cost.
537	$EENS_y$	Expected energy not supplied at stage y .
	$f_{ij,y}^{SO}$	Flow across branch ij of the fictitious system used at stage y to compute $\Gamma_{i,y}^{SO}$.
	$I_{ij,c,l,y}$	Magnitude of the current across branch ij for conductor type c , load level l , and stage y .
	$I_{ij,c,l,y}^{sqr}$	Squared magnitude of the current across branch ij for conductor type c , load level l , and stage y .
	$\hat{I}_{ij,l,y}^{sqr}$	Squared magnitude of the current across branch ij for load level l and stage y .
	$P_{ij,c,l,y}, Q_{ij,c,l,y}$	Active and reactive power flows across branch ij for conductor type c , load level l , and stage y .
538	$\hat{P}_{ij,l,y}, \hat{Q}_{ij,l,y}$	Active and reactive power flows across branch ij for load level l and stage y .
	$P_{i,l,y}^S, Q_{i,l,y}^S$	Active and reactive power injections at substation node i , load level l , and stage y .
	$P_{i,l,y}^{Sh}, Q_{i,l,y}^{Sh}$	Active and reactive load shedding at node i , load level l , and stage y .
	$Q_{i,l,y}^{CB}$	Reactive power injection of the capacitor bank at node i , load level l , and stage y .
	$S_{i,l,y}^{S,sqr}$	Squared value of the apparent power injected at substation node i , load level l , and stage y .
	$V_{i,l,y}$	Voltage magnitude at node i , load level l , and stage y .
	$V_{i,l,y}^{sqr}$	Squared voltage magnitude at node i , load level l , and stage y .
	<i>Binary Variables</i>	
	$x_{ij,c,y}^{AB}, x_{ij,c,y}^{RB}$	Investment variables for conductor type c for candidate and replaceable branch ij at stage y .
	$x_{i,y}^S$	Investment variable for the substation at node i and stage y .
539	$x_{i,t,y}^T, w_{i,t,y}^T$	Investment and operational variables for alternative t for new transformers at substation node i and stage y .
	$w_{ij,c,y}^B$	Operational variable for conductor type c for branch ij at stage y .
	$w_{ij,y}^{B+}, w_{ij,y}^{B-}$	Forward and backward directions of the flow across branch ij at stage y .
	$w_{i,y}^{S,ex}$	Operational variable for the existing substation at node i and stage y .

540 **B. Linearization Schemes**

541 The linearization schemes used in Section 3 are described next.

542 *B.1. Linearization of the Quadratic Terms in (35) and (41)*

For expository purposes, the quadratic terms in (35) and (41) are represented by the generic form z^2 , where z is a continuous variable. If z denotes a variable that can take both positive and negative values, the linearization is reduced to the positive orthant, i.e., $|z|^2$ is linearized rather than z^2 . According to [39], $|z|$ can be equivalently represented by the sum of two auxiliary non-negative variables z^+ and z^- complying with the following set of linear constraints:

$$z^+ - z^- = z \tag{B.1}$$

$$0 \leq z^+ \leq \bar{z} \tag{B.2}$$

$$0 \leq z^- \leq \bar{z} \tag{B.3}$$

543 where \bar{z} is the upper bound for $|z|$.

544 The piecewise linearization thus comprises two steps:

- 545 1. The replacement of z^2 in (35) and (41) with $\sum_{\kappa=1}^K \sigma_{z,\kappa} \Delta_{z,\kappa}$, where K is the number of blocks
 546 into which $|z|$ is discretized, $\sigma_{z,\kappa}$ is the slope of $|z|^2$ in the κ th block, and $\Delta_{z,\kappa}$ is a continuous
 547 variable representing the contribution of the κ th block to the value of $|z|$. The slopes are
 548 defined as $\sigma_{z,\kappa} = \frac{1}{\bar{\Delta}_{z,\kappa}} \left[\left(\sum_{\nu=1}^{\kappa} \bar{\Delta}_{z,\nu} \right)^2 - \left(\sum_{\nu=1}^{\kappa-1} \bar{\Delta}_{z,\nu} \right)^2 \right]$, $\kappa = 1, \dots, K$, where $\bar{\Delta}_{z,\kappa}$ is the width
 549 of the κ th block.
2. The incorporation of (B.1)–(B.3) and the following constraints:

$$z^+ + z^- = \sum_{\kappa=1}^K \Delta_{z,\kappa} \tag{B.4}$$

$$0 \leq \Delta_{z,\kappa} \leq \bar{\Delta}_{z,\kappa}; \kappa = 1, \dots, K. \tag{B.5}$$

550 The relationship between z^+ , z^- , and $\Delta_{z,\kappa}$ is modeled in (B.4) whereas the upper and lower
 551 bounds for variables $\Delta_{z,\kappa}$ are set in (B.5).

552 Note that if z denotes a non-negative variable, auxiliary variables z^+ and z^- and constraints
 553 (B.1)–(B.3) are no longer needed and the left-hand side of (B.4) can be replaced with z .

554 *B.2. Linearization of the Products of Two Binary Variables in (49)*

555 A linear equivalent for the product of two binary variables $x \in \{0, 1\}$ and $y \in \{0, 1\}$ is obtained
 556 as follows [40]:

- 557 1. Replace the product xy with a new binary variable z .
2. Introduce the following new expressions:

$$z \in \{0, 1\} \tag{B.6}$$

$$z \leq x \tag{B.7}$$

$$z \leq y \tag{B.8}$$

$$z \geq x + y - 1. \tag{B.9}$$

558 Expression (B.6) imposes the integrality of the newly added binary variable z . Expressions
 559 (B.6)–(B.8) make sure that if either x or y is equal to 0, the new binary variable z is also equal to
 560 0. Analogously, expressions (B.7)–(B.9) ensure that z is equal to 1 if both binary variables, x and
 561 y , are equal to 1.

562 Acknowledgments

563 The work of A. Tabares and J. F. Franco was funded in part by the Coordination for the
564 Improvement of Higher Education Personnel - Brazil (CAPES) - Finance Code 001 (process No.
565 88881.134450/2016-01), the São Paulo Research Foundation (FAPESP) (grant 2017/02831-8, 2018/
566 20990-9), and the Brazilian National Council for Scientific and Technological Development (CNPq)
567 (processes No. 152002/2016-2 and 313047/2017-0). The work of G. Muñoz-Delgado, J. M. Arroyo,
568 and J. Contreras was supported by the Ministry of Science, Innovation and Universities of Spain,
569 under Projects RTI2018-096108-A-I00 and RTI2018-098703-B-I00 (MCIU/AEI/FEDER, UE).

570 References

- 571 [1] R. Billinton, R. N. Allan, Reliability Evaluation of Power Systems, New York, NY, USA:
572 Plenum Press, 1996.
- 573 [2] R. Billinton, P. Wang, Reliability-network-equivalent approach to distribution-system-
574 reliability evaluation, *IEE Proc.-Gener. Transm. Distrib.* 145 (1998) 149–153.
- 575 [3] IEEE Guide for Electric Power Distribution Reliability Indices, 2012.
- 576 [4] R. E. Brown, Electric Power Distribution Reliability, 2nd ed., Boca Raton, FL, USA: CRC
577 Press, 2008.
- 578 [5] S. Conti, R. Nicolosi, S. A. Rizzo, Generalized systematic approach to assess distribution
579 system reliability with renewable distributed generators and microgrids, *IEEE Trans. Power*
580 *Deliv.* 27 (2012) 261–270.
- 581 [6] G. T. Heydt, T. J. Graf, Distribution system reliability evaluation using enhanced samples in
582 a Monte Carlo approach, *IEEE Trans. Power Syst.* 25 (2010) 2006–2008.
- 583 [7] E. G. Carrano, F. G. Guimarães, R. H. C. Takahashi, O. M. Neto, F. Campelo, Electric distri-
584 bution network expansion under load-evolution uncertainty using an immune system inspired
585 algorithm, *IEEE Trans. Power Syst.* 22 (2007) 851–861.
- 586 [8] R. C. Lotero, J. Contreras, Distribution system planning with reliability, *IEEE Trans. Power*
587 *Deliv.* 26 (2011) 2552–2562.
- 588 [9] I. Ziari, G. Ledwich, A. Ghosh, G. Platt, Optimal distribution network reinforcement consid-
589 ering load growth, line loss, and reliability, *IEEE Trans. Power Syst.* 28 (2013) 587–597.
- 590 [10] B. R. Pereira, Jr., A. M. Cossi, J. Contreras, J. R. S. Mantovani, Multiobjective multistage
591 distribution system planning using tabu search, *IET Gener. Transm. Distrib.* 8 (2014) 35–45.
- 592 [11] G. Muñoz-Delgado, J. Contreras, J. M. Arroyo, Multistage generation and network expansion
593 planning in distribution systems considering uncertainty and reliability, *IEEE Trans. Power*
594 *Syst.* 31 (2016) 3715–3728.
- 595 [12] C. Wang, T. Zhang, F. Luo, P. Li, L. Yao, Fault incidence matrix based reliability evaluation
596 method for complex distribution system, *IEEE Trans. Power Syst.* 33 (2018) 6736–6745.
- 597 [13] J. C. López, M. Lavorato, M. J. Rider, Optimal reconfiguration of electrical distribution
598 systems considering reliability indices improvement, *Int. J. Electr. Power Energy Syst.* 78
599 (2016) 837–845.

- 600 [14] G. Muñoz-Delgado, J. Contreras, J. M. Arroyo, Reliability assessment for distribution opti-
601 mization models: A non-simulation-based linear programming approach, *IEEE Trans. Smart*
602 *Grid* 9 (2018) 3048–3059.
- 603 [15] A. Tabares, G. Muñoz-Delgado, J. F. Franco, J. M. Arroyo, J. Contreras, An enhanced algebraic
604 approach for the analytical reliability assessment of distribution systems, *IEEE Trans. Power*
605 *Syst.* 34 (2019) 2870–2879.
- 606 [16] M. Jooshaki, A. Abbaspour, M. Fotuhi-Firuzabad, G. Muñoz-Delgado, J. Contreras, M. Lehto-
607 nen, J. M. Arroyo, Linear formulations for topology-variable-based distribution system reli-
608 ability assessment considering switching interruptions, *IEEE Trans. Smart Grid* 11 (2020)
609 4032–4043.
- 610 [17] Z. Li, W. Wu, B. Zhang, X. Tai, Analytical reliability assessment method for complex distri-
611 bution networks considering post-fault network reconfiguration, *IEEE Trans. Power Syst.* 35
612 (2020) 1457–1467.
- 613 [18] Z. Li, W. Wu, X. Tai, B. Zhang, Optimization model-based reliability assessment for distri-
614 bution networks considering detailed placement of circuit breakers and switches, *IEEE Trans.*
615 *Power Syst.* 35 (2020) 3991–4004.
- 616 [19] G. Muñoz-Delgado, J. Contreras, J. M. Arroyo, Distribution network expansion planning with
617 an explicit formulation for reliability assessment, *IEEE Trans. Power Syst.* 33 (2018) 2583–2596.
- 618 [20] M. Jooshaki, A. Abbaspour, M. Fotuhi-Firuzabad, H. Farzin, M. Moeini-Aghaie, M. Lehtonen,
619 A MILP model for incorporating reliability indices in distribution system expansion planning,
620 *IEEE Trans. Power Syst.* 34 (2019) 2453–2456.
- 621 [21] M. Jooshaki, A. Abbaspour, M. Fotuhi-Firuzabad, M. Moeini-Aghaie, M. Lehtonen, MILP
622 model of electricity distribution system expansion planning considering incentive reliability
623 regulations, *IEEE Trans. Power Syst.* 34 (2019) 4300–4316.
- 624 [22] Z. Li, W. Wu, B. Zhang, X. Tai, Feeder-corridor-based distribution network planning model
625 with explicit reliability constraints, *IET Gener. Transm. Distrib.* 14 (2020) 5310–5318.
- 626 [23] Z. Li, W. Wu, X. Tai, B. Zhang, A reliability-constrained expansion planning model for mesh
627 distribution networks, *IEEE Trans. Power Syst.* 36 (2021) 948–960.
- 628 [24] A. Tabares, J. F. Franco, M. Lavorato, M. J. Rider, Multistage long-term expansion planning
629 of electrical distribution systems considering multiple alternatives, *IEEE Trans. Power Syst.*
630 31 (2016) 1900–1914.
- 631 [25] J. A. Taylor, F. S. Hover, Convex models of distribution system reconfiguration, *IEEE Trans.*
632 *Power Syst.* 27 (2012) 1407–1413.
- 633 [26] A. R. Jordehi, Optimisation of electric distribution systems: A review, *Renew. Sust. Energ.*
634 *Rev.* 51 (2015) 1088–1100.
- 635 [27] H. L. Willis, *Power Distribution Planning Reference Book*, 2nd ed., New York, NY, USA:
636 Marcel Dekker, 2004.
- 637 [28] P. S. Georgilakis, N. D. Hatziargyriou, A review of power distribution planning in the modern
638 power systems era: Models, methods and future research, *Electr. Power Syst. Res.* 121 (2015)
639 89–100.

- 640 [29] G. L. Nemhauser, L. A. Wolsey, *Integer and Combinatorial Optimization*, New York, NY, USA:
641 Wiley-Interscience, 1999.
- 642 [30] K. B. Debnath, M. Mourshed, Forecasting methods in energy planning models, *Renew. Sust.*
643 *Energ. Rev.* 88 (2018) 297–325.
- 644 [31] L. Blank, A. Tarquin, *Engineering Economy*, 7th ed., New York, NY, USA: McGraw-Hill, 2012.
- 645 [32] S. Haffner, L. F. A. Pereira, L. A. Pereira, L. S. Barreto, Multistage model for distribution
646 expansion planning with distributed generation—Part I: Problem formulation, *IEEE Trans.*
647 *Power Deliv.* 23 (2008) 915–923.
- 648 [33] J. F. Franco, M. J. Rider, M. Lavorato, R. Romero, A mixed-integer LP model for the re-
649 configuration of radial electric distribution systems considering distributed generation, *Electr.*
650 *Power Syst. Res.* 97 (2013) 51–60.
- 651 [34] M. E. Baran, F. F. Wu, Optimal capacitor placement on radial distribution systems, *IEEE*
652 *Trans. Power Deliv.* 4 (1989) 725–734.
- 653 [35] M. Lavorato, J. F. Franco, M. J. Rider, R. Romero, Imposing radiality constraints in distribu-
654 tion system optimization problems, *IEEE Trans. Power Syst.* 27 (2012) 172–180.
- 655 [36] A. Tabares, G. Muñoz-Delgado, J. F. Franco, J. M. Arroyo, J. Contreras, Electronic
656 companion—Multistage reliability-based expansion planning of ac distribution networks using
657 a mixed-integer linear programming model: System data and results, 2021. URL: <https://github.com/tabarespozos/Reliability-Based-DNEP.git>, accessed 2021-01-16.
- 658 <https://github.com/tabarespozos/Reliability-Based-DNEP.git>, accessed 2021-01-16.
- 659 [37] GAMS Development Corporation, 2021. URL: <http://www.gams.com>, accessed 2021-01-16.
- 660 [38] J. F. Franco, M. J. Rider, R. Romero, A mixed-integer quadratically-constrained programming
661 model for the distribution system expansion planning, *Int. J. Electr. Power Energy Syst.* 62
662 (2014) 265–272.
- 663 [39] D. Bertsimas, J. N. Tsitsiklis, *Introduction to Linear Programming*, Belmont, MA, USA:
664 Athena Scientific, 1997.
- 665 [40] F. Glover, E. Woolsey, Converting the 0-1 polynomial programming problem to a 0-1 linear
666 program, *Oper. Res.* 22 (1974) 180–182.